Molecular Dynamics Simulation of Plane Poiseuille Flow in Nanochannels

Valery Ya. RUDYAK[1,2,*], Aleksandr A. BELKIN[2], Veniamin V. EGOROV [2], Denis A. IVANOV[2]

* Corresponding author: Tel.: 83832668014; Email: valery.rudyak@mail.ru
1 Baker Huges Inc., Russian Science Center, Novosibirsk, Russia
2 Novosibirsk State University of Architecture and Civil Engineering, Novosibirsk, Russia

Abstract This paper presents new techniques and results of simulating microflows in plane channels by the molecular dynamics (MD) method. Mass forces and thermostat are not used in these techniques. The flows are simulated by both hard-sphere molecules and molecules with the Lennard-Jones intermolecular potential. Flow at a given fluid flow rate is implemented. In this case, the initial shock profile is transformed to a parabolic type profile. However, unlike in ordinary Poiseuille flows, a slip effect is recorded on the channel walls. It is shown that, in a nanochannel, a linear pressure gradient occurs. Fluid structuring is studied. The effects of fluid density, accommodation coefficients, and channel dimensions on flow properties are investigated.

Keywords: Nanochannels, Plane Poiseuille Flow, Pressure Gradient, Molecular Dynamics Simulation

1. Introduction

The importance of investigating fluid flows in micro- and nanochannels is due primarily to the rapid development of MEMS- and nano-technologies. Experimental studies of such flows are complicated by their small sizes, and molecular dynamics (MD) simulation is an alternate method of research. The first MD simulations were carried out more than twenty years ago (see, for example Koplik, Banavar and Willemsen, 1989; Heinbuch and Fischer, 1989; Karniadakis, Beskok and Aluru, 2005 and the references therein). Directional motion of a fluid in a nanochannel is usually produced by using an artificial external mass force. This force is often called the gravitational force, but it is hundreds times higher than the characteristic values of gravity (see, for example, Karniadakis, Beskok and Aluru, 2005). Because the action of the external force leads to a continuous increase in the flow velocity and temperature, it is necessary to additionally stabilize the system. This is done by means of the so-called thermostat or other methodic (Hoover, 1985), which are, in essence, a numerical technique which does not have a real physical analog. The introduction of such a mass force is not suitable for simulating real microflows generated by a pressure difference along the channel or a specified flow rate at the entrance.

This paper presents new MD techniques for simulating Poiseuille-type flows in micro- and nanochannels and the results of simulation of such flows obtained using these techniques.

The channel walls and the fluid flow are modeled by two different methods. In the first case, the channel walls are modeled by several rows of molecules and the interaction of fluid molecules with each other and with the molecules of the walls are described by the Lennard-Jones (LJ) potential. In the second case, the hard spheres law is used to simulate molecule-molecule interaction, molecule-wall interaction is described by the specular, diffuse, and specular-diffuse reflection laws.

2. Microflows simulation techniques

We consider fluid flow between two solid parallel surfaces, which is an analog of classical hydrodynamic plane Poiseuille flow. In practice, the characteristic length of such a channel is much greater than its height (the channel width is infinite). In typical microflows, the channel height is $h \sim 1 \div 300$ μm and its length $L \sim 1$ cm (see, for example, Tabeling, 2005). The nanochannel height does

not exceed 100 nm. To satisfy these conditions, we used a rectangular simulation cell with length L greater than its height h. The cell width was varied. Along this direction, the usual periodic conditions were employed (see, for example, Rapaport, 2005).

The difficulties in MD simulations of micro- and nanoflows are due to several factors:

- the presence of, at least, two significantly different flow scales;
- the necessity of developing a technique for modeling steady-state flows;
- the necessity of developing an adequate technique for modeling the interaction of molecules with the solid surfaces bounding the flow.

Because for the MD simulations we used systems of molecules with different interaction potentials, the simulation techniques developed were also somewhat different. They are briefly described below.

In the case where the flow was modeled by hard-sphere molecules, the upper and lower boundaries of the computational cell were modeled by smooth surfaces. In this case the interaction of molecules with the solid surfaces was described by the specular or specular-diffuse laws of reflection. For diffuse reflection, the molecular velocity after collision with the wall was given by the Maxwell distribution. In particular, the absolute value of the velocity v and the velocity projection v_z onto the z axis perpendicular to the wall were defined by the relations

$$f(v) = 4\pi v^2 \left(\frac{m}{2\pi kT}\right)^{\frac{3}{2}} \exp\left(-\frac{mv^2}{2kT}\right),$$

$$f(v_z) = \left(\frac{m}{2\pi kT}\right)^{\frac{1}{2}} \exp\left(-\frac{mv_z^2}{2kT}\right), \qquad (1)$$

where T is the temperature of the system, k is Boltzmann's constant, and m is the molecular mass.

In specular-diffuse reflection, some fraction of the molecules θ is diffuse reflected and the remaining molecules are specularly reflected. The fraction of diffuse-reflected molecules is in fact the accommodation coefficient of the tangential momentum component, so that $\theta = 0$ for specular reflection and $\theta = 1$ for diffuse reflection.

As noted above, systems of molecules with the truncated LJ intermolecular potential

$$\Phi(r) = \begin{cases} 4\varepsilon\left[(\sigma/r)^{12} - (\sigma/r)^{6}\right], & r \le R \\ 0, & r > R \end{cases}. \qquad (2)$$

are also used to simulate microflows. Here R is the truncation radius and $r = |\mathbf{r}_i - \mathbf{r}_j|$ is the distance between the molecules i and j. In the calculations presented here, $R = 2.5\sigma$. The upper and lower surfaces of the channel were modeled by two layers of fixed close-packed molecules. The interaction between the fluid molecules was modeled by the LJ potential (2). The interaction between the molecules of the fluid and the wall was also described by the LJ potential but with different values of the parameters σ and ε.

2.1 Techniques I. Pseudo-periodic conditions

The conditions at the left and right boundaries of the simulation cell depended on the flow implementation method. Three different techniques were developed. In the first technique, channel flow is sustained by quasi-periodic boundary conditions (see Fig.1). At the initial time, the molecules are arranged uniformly in the simulation cell and their velocities are given by the Maxwell distribution. The right boundary of the channel is open to the molecules (see Fig. 1). When a molecule reaches this boundary, its copy appears at the left boundary (channel entrance). At the time the molecule leaves the channel, its copy completely enters the channel. The velocity of the incoming molecule differs from that of the outgoing molecule, and the velocity components are calculated from the Maxwell distribution (1) at a given temperature. In addition, the velocity projection of the incoming molecule onto the axis parallel to the channel axis is always defined positively. We note that the molecules cannot leave the channel through the left boundary. They are reflected specularly or

diffusely from this boundary at a given temperature. After a time determined by the channel length, a steady-state flow at a given hydrodynamic velocity u along the channel is established.

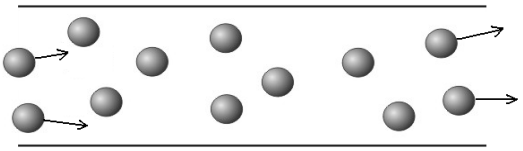

Fig. 1. Diagram of plane flow with pseudo-periodic boundary conditions.

In this model, the number of molecules in the channel remains constant. This is convenient from a point of view of software implementation. In this case, however, it is impossible to control the fluid flow rate. In addition, there is nonphysical long-range molecular interaction – molecules at the right boundary (exit) interact with molecules at the left boundary.

2.2 Techniques II. Flow with given flow rate

For the hard-sphere model, plane flow at a given flow rate is implemented as follows. A definite number of molecules ΔN (Fig. 2) given by the relation $\Delta N = nhwd$ (n is the number density of molecules, d is their diameter, h and w are the height and width of the cell) are introduced into the channel through the left boundary (channel entrance) at equal time intervals Δt. This layer of molecules moves translationally as a rigid body at a constant velocity v_x^*. After the x coordinates of the introduced molecules became equal to $x = d/2$, each of them are assigned definite values of the mass m and velocity $(\mathbf{v} + u\mathbf{i})$. Here **i** is the unit vector along the channel axis x, the velocity **v** is given by distribution (1), and the value of u is set constant. Thus, a so-called shock profile with the average velocity u is formed at the entrance (see Section 3). With time, this profile transforms to a developed Poiseuille profile and steady flow is established in the channel. For the LJ system of molecules, the flow is implemented similarly.

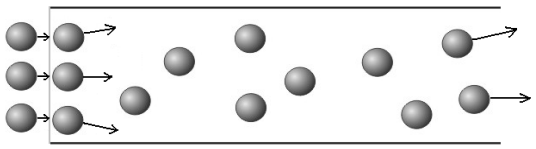

Fig. 2. Diagram of plane flow at a given flow rate.

2.3. Techniques III. Flow with given flow rate and controlled fluid density

In the technique described in the previous section, the fluid molecules are free to pass through the channel exit. As a result, a zone with a reduced concentration of molecules forms at the right boundary. Thus, in a channel of given length L, steady-state flow with a given fluid density occurs only on a length $l < L$. The reduction in the molecular concentration at a constant fluid flow rate leads to an increase in the mean molecular velocity, which is not typical for real stationary hydrodynamic flows.

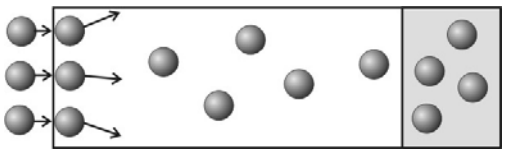

Fig. 3. Diagram of plane flow at a given flow rate and controlled fluid density.

In a real device, if fluid is free to flow from the microchannel into vacuum (or into zone of lower pressure), this effect always occurs. In this case, technique II models the real situation. If a microchannel is terminated by a reservoir with a given concentration of molecules, the technique should be modified.
For this, at the right boundary (channel exit) of the simulation cell, a region (reservoir, see Fig. 3) is distinguished in which the molecular concentration (and/or the fluid pressure) is controlled. When one of the molecules reaches the right boundary of the channel, the molecular concentration in the reservoir is measured. If it is found to be higher than a certain value, the molecule leaves the channel; otherwise, it is reflected back as from an elastic wall. Physically, this model corresponds to a valve which opens only at a high pressure at the channel entrance.

3. Some features of fluid flows in nanochannels

3.1. Pressure gradient and flow velocity

As we mentioned above, a shock velocity profile occurs in channel flow at a given flow rate at the entrance (see Fig. 4). As the fluid moves in a macroscopic channel, the shock profile transforms to a parabolic one. This transformation is due to wall friction. Hence, the use of no-slip boundary conditions for the Navier–Stokes equations corresponds to similar macroscopic flow. In MD simulations of plane-channel flow, the velocity characteristics are determined by the molecule–wall interaction law. If specular interaction is used, the tangential momentum of the molecules does not change and the shock velocity profile remains unchanged. In the case of diffuse or specular-diffuse interaction of molecules with the wall, the initial shock profile is transformed to a parabolic-type profile. This process is shown in Fig. 4 for fluid with density $\beta = nd^3 = 0.283$. The region of the velocity profile transformation has a size of order kh, where k is a number that depends on the accommodation coefficient.

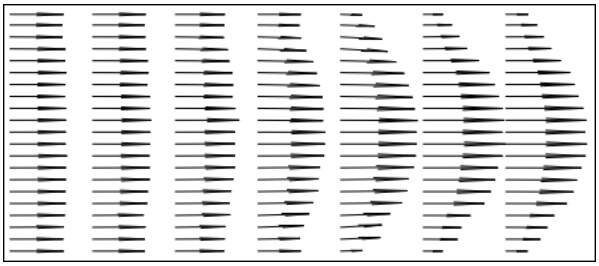

Fig. 4. Fragment of the velocity field in a nanochannel for the channel height $h = 6d$, and $\theta = 1$.

A typical velocity profile is presented in Fig. 5. Here the MD simulation results are shown by crosses and a parabolic approximation of the simulated data is shown by the solid curve. Thus, the flow velocity profile formed in micro- and nanochannels is parabolic, as in the case of usual macroscopic channels. This profile, however, is not a usual Poiseuille profile because the flow velocity is not equal to zero on the walls and the slip effect occurs. This result is in qualitative agreement with data of other authors (see, for example, Koplik, Banavar and Willemsen, 1989; Karniadakis, Beskok and Aluru, 2005).

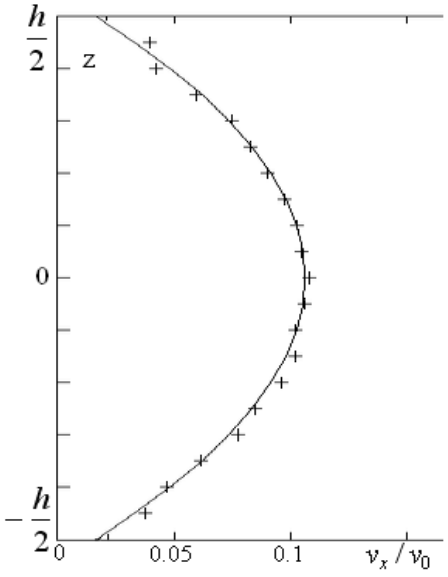

Fig. 5. Velocity profile of developed flow in a nanochannel. $\beta = 0.283$, $h = 6d$, and $\theta = 1$.

In micro- and nanochannels, the flow velocity near the walls never vanishes even for an accommodation coefficient equal to unity (purely diffuse reflection). Physically, this behavior is quite clear. Indeed, the mean x component of the velocity is equal to zero for the molecules reflected from the wall in diffuse reflection. However, molecules with nonzero x component of the velocity (which do not interact with the wall) exist near the wall. Therefore, the mean flow velocity of the molecules along the channel is always different from zero. One should not think that the slip length in fluid flow is always of the order of several d. First, the slip length depends markedly on the accommodation coefficient of the surface. It increases with decreasing accommodation coefficient. Second, a decrease in the fluid density also leads to an increase in the slip length. Third, the slip length depends on the degree of surface smoothness. In channels, the height of roughness elements even on fairly smooth surfaces can vary from a few nanometers to a few microns. This can also increase the slip length (however, one can imagine a situation

in which, conversely, the presence of surface roughness decreases the slip length due to an increase in the effective interaction surface for the molecules).

Finally, the fluid structure changes significantly at the surface. In fluids, the characteristic size of the bulk short-range order is on the order of a nanometer. In fact, this size determines the scale of the correlations existing in fluids under ordinary conditions. If the structure of the fluid at the wall remained unchanged, the slip length would not exceed $1 \div 2$ *nm*. However, the near-surface fluid structure differs from the structure of the bulk fluid. As a result, the slip length may be much greater. Available experimental data indicate that the slip length can be a few microns and even a few hundred microns (see Lauga, Brenner and Stoneet, 2005).

The MD method can be used to study flows in channels of various sizes, but to calculate the actual slip length, one needs to simulate flow in a channel with $h >> d$. Generally, the slip length in nanochannels can be smaller than that in microchannels because of screening effects and fluid structuring, which will be discussed below.

The MD simulation procedures described in the previous section have made it possible for the first time to obtain dependences of flow characteristics not only on the transverse coordinate (i.e. at a given channel cross section) but also on the longitudinal coordinate. Therefore not only velocity, density, etc. profiles but also their fields along the entire channel have been obtained. In particular, real plane Poiseuille-type flow at a given flow rate or with a constant pressure gradient along the channel has been simulated for the first time. In such flow, the pressure decreases linearly due to wall friction. The pressure drop in a typical MD simulation is presented in Fig. 6. Here p_0 is the pressure at the channel entrance. As in hydrodynamic flow, the pressure drop is described by a linear law. In hydrodynamic flow, the pressure drop is determined by the fluid viscosity. In micro- and nanochannel flows, it is caused by the loss of the tangential momentum due to molecule–wall interaction. In this case, therefore, the pressure drop depends on the accommodation coefficient and increases with its increase (see Fig. 6). The maximum pressure drop occurs for $\theta = 1$.

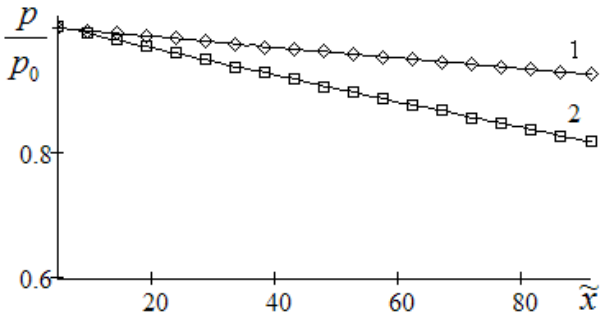

Fig. 6. Pressure averaged over the channel cross section versus dimensionless longitudinal coordinate $\tilde{x} = x/d$. Straight lines 1 and 2 correspond to computations approximation, $\theta = 0.3$, and $\theta = 1$, respectively.

3.2. Concentration of the fluid molecules

One of the most interesting phenomena observed in nanochannel flows is fluid structuring. The structuring effect was noted even in early papers on MD simulation of channel flows (see, for example, Bocquet and Barrat, 1994 and the references therein). Typical behavior of the fluid density profile is presented in Fig. 7. This behavior is slightly different for hard spheres and LJ molecules. In particular, there are differences between the density profiles near the walls. They are caused by the screening effect; unlike LJ molecules, hard spheres cannot come closer to the wall than the sphere radius.

The concentration profiles presented in Fig. 7 are typical of all molecular dynamics studies of the behavior of microflows. However, no information has so far been obtained on the density variation along the channel. Figure 8 gives the fluid concentration field for flow in a nanochannel of height $h = 6d$ and length $L = 72d$. In the figure, the concentration is normalized by the mean concentration of fluid molecules. A characteristic feature of the flow presented in Fig. 8 is the formation of distinct layers with high and low concentrations of the molecules. Because the fluid in the channel is rather dense and its height is not great, regions are formed which are inaccessible to the molecules (screening effect). The existence of

velocity along the channel orders the structures formed, resulting in the occurrence of the next downstream layers.

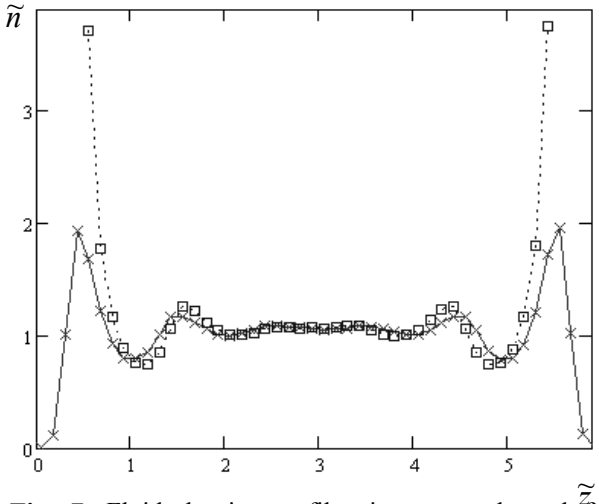

Fig. 7. Fluid density profiles in a nanochannel for Lennard-Jones molecules (×) and the hard-sphere model for $\theta = 0.3$ (□), $\beta = 0.471$, and $h = 6d$.

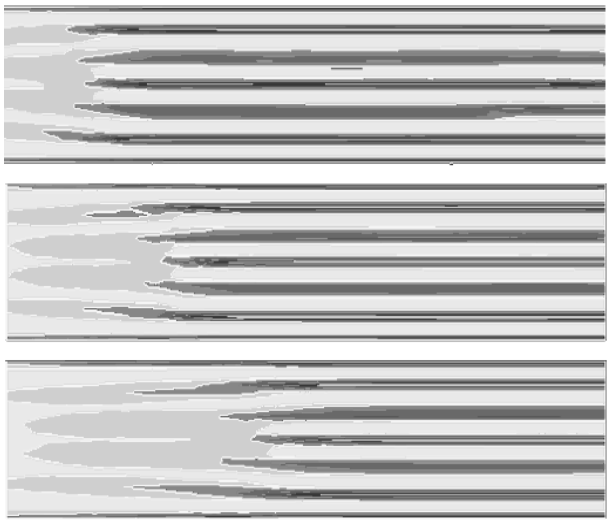

Fig. 8. Molecular concentration fields in a plane channel for various accommodation coefficients (from top to bottom) $\theta = 1$, $\theta = 0.75$, and $\theta = 0.5$ ($\beta = 0.707$, $h = 6d$, and $L = 72d$).

The formation of the layered structure indicates that the thermal motion of the molecules in the channel cross section is hindered. In a narrow nanochannel, there is a transition of the molecular system from the fluid state to a special ordered state. In the process, the fluid viscosity increases considerably, resulting in partial channel blocking. It should be emphasized that, for a fluid of a given density, fluid structuring has a threshold nature and is observed only beginning at a certain characteristic channel height. As the channel height is increased by a factor of two, to $12.2d$, the pronounced fluid structuring disappears practically.

On the other hand fluid structuring in channels is greatly affected by the fluid density. In channel flows, the lower fluid density, the later fluid structuring begins. As noted above, structuring is partially a geometrical effect; in narrow channels, molecules can be arranged only in a definite manner. As the density decreases, "the number of degrees of freedom" of the system increases and structuring is observed at much later stages of the flow evolution.

One can say that there is a transition from the usual bulk short-range order to long-range order, caused by the interaction with the boundary. The latter is illustrated in Fig. 8. Decreasing the accommodation coefficients produces almost the same effect as decreasing the fluid density; as the coefficient θ decreases, the layered fluid structure begins to form at a greater distance from the channel entrance. In particular, this indicates that structuring is not only a geometrical effect.

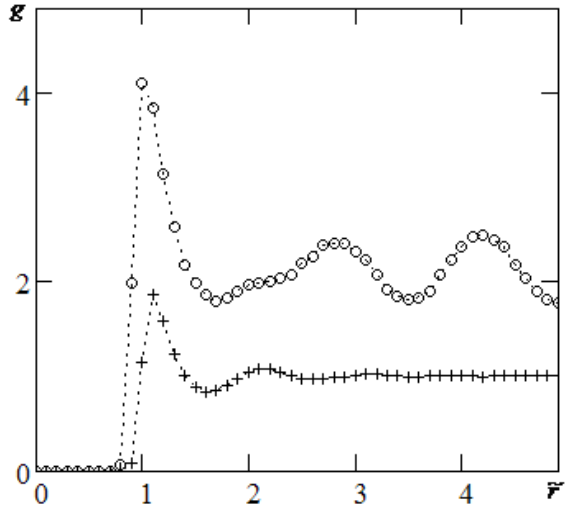

Fig. 9. Radial distribution function g of fluid molecules in bulk (+) and in nanochannel (○). $\tilde{r} = r / d$.

In a relatively wide channel, as noted above, fluid structuring over the entire channel height is absent. However the behavior of the density near the channel walls is not almost depended

on the height of the channel. It is important to emphasize that structure of the fluid in bulk and near the hard surfaces is very different. In Fig. 9 the radial distribution functions of the fluid in bulk and near the wall are compared. Here the fluid density is equal to $\beta = 0.707$ and the channel height is equal to $h = 6d$. Radial distribution function of the fluid in the channel is calculated for the $r = (0.48 \div 0.52)d$ from its wall. Thus the fluid near the wall is more ordered. The characteristic range of the fluid short-order in bulk and near the hard surface is rather different.

A characteristic feature of nanoflows is fluid compressibility. The structuring described above indicates that the fluid density is not uniform in the channel cross section. In addition, it also varies along the channel if, of course, the special actions are not used (see the techniques III from Section 2). The fluid molecule concentration decreases along the channel. This is observed in both the diffuse interaction of fluid molecules with the channel walls and the interaction via the LD potential.

In fact, this effect has a threshold nature. It can be ignored if the momentum imparted to the molecules by the walls is much smaller than their total momentum. This is true for macroscopic flows.

Conclusions

The MD techniques proposed in the present paper allows simulations of real plane microflows at a given fluid flow rate at the entrance. They are easily extended to flows in microchannels of cylindrical or rectangular cross sections. These techniques are suitable for investigating the real properties of microflows and their transformation along the channel axis. It is possible to study variations in the fluid pressure and density and the mean flow velocity along the channel.

A characteristic property of microflows is the observed nonuniformity of fluid density. Fluids in nanochannels are compressible with the molecular concentration reducing along the channel. This reduction is due to the molecule–wall interaction, and it can be ignored only when the number of molecules interacting with the wall is much smaller than the number of molecules in the bulk of the channel. The reduction in the molecular concentration along the channel at a constant flow rate leads to an increase in the mean molecular velocity, which is not typical of macroscopic flows. This effect should be observable experimentally.

Fluid structuring in nanochannels is the most important factor of nanoflows. Such structuring is not observed in microflows, where the channel height is tens and hundreds of microns. However, the fluid near the boundaries of micro- and nanochannels are always different in structure from the bulk fluid. This leads to differences in transfer properties between the bulk and the flow boundaries. This refers, in particular, to fluid viscosity and, possibly, thermal conductivity.

Acknowledgement

This work was supported in part by the Russian Foundation for Basic Researches (grant No. 07-08-00164) and by the grant of the President of the Russian Federation for Support of Leading Scientific Schools (project no. NSh-454.2008.1).

References

Koplik, J., Banavar, J.R., Willemsen, J.F., 1989. Molecular Dynamics of Fluid Flow at Solid Surfaces. Phys. Fluids A. **1**, 781–794.

Heinbuch, U., Fischer, J., 1989. Liquid flow in pores: Slip, non-slip, or multilayer sticking. Phys. Rev. A. **40**, 1144–1146.

Karniadakis, G., et al., 2005. Microflows and Nanoflows. In: Interdisciplinary Appl. Math. **29**.

Hoover, W.G., Canonical dynamics: Equilibrium phase-space distributions. 1985. Phys. Rev. A. **31**, 1695 – 1697.

Tabeling, P., 2005. Introduction to microfluidics. Oxford University Press.

Rapaport, D.C., 2005. The art of molecular dynamics simulation. Cambridge University Press.

Lauga, E., et al., 2005. Microfluidics: the no-slip boundary condition. In: Handbook of Exper. Fluid Dynamics. Springer.

Bocquet, L., Barrat, J., 1994. Hydrodynamic boundary conditions, correlation functions, and Kubo relations for confined fluid. Phys. Rev. E. **49**, 3079–3092